

An assessment of the optimal scale for monitoring of MODIS and FIA NPP across the eastern USA

Youngsang Kwon & Chris P. S. Larsen

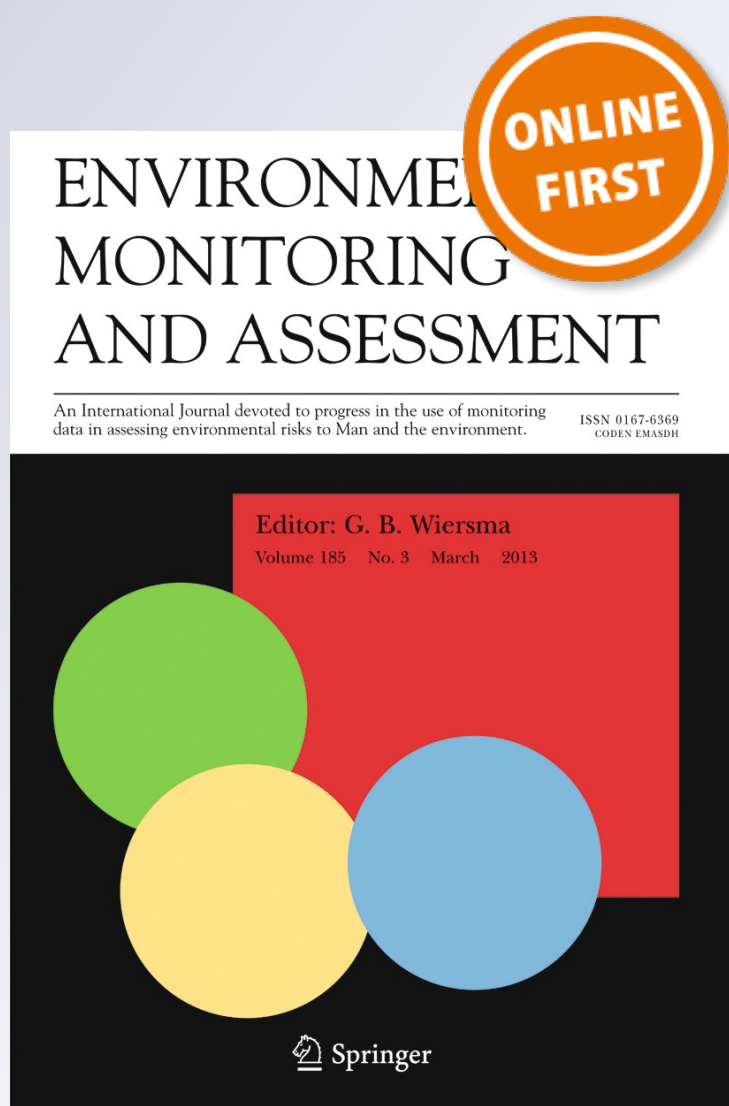
Environmental Monitoring and Assessment

An International Journal Devoted to Progress in the Use of Monitoring Data in Assessing Environmental Risks to Man and the Environment

ISSN 0167-6369

Environ Monit Assess

DOI 10.1007/s10661-013-3099-1



Your article is protected by copyright and all rights are held exclusively by Springer Science +Business Media Dordrecht. This e-offprint is for personal use only and shall not be self-archived in electronic repositories. If you wish to self-archive your work, please use the accepted author's version for posting to your own website or your institution's repository. You may further deposit the accepted author's version on a funder's repository at a funder's request, provided it is not made publicly available until 12 months after publication.

An assessment of the optimal scale for monitoring of MODIS and FIA NPP across the eastern USA

Youngsang Kwon · Chris P. S. Larsen

Received: 17 August 2012 / Accepted: 15 January 2013
© Springer Science+Business Media Dordrecht 2013

Abstract Robust monitoring of carbon sequestration by forests requires the use of multiple data sources analyzed at a common scale. To that end, model-based Moderate Resolution Imaging Spectroradiometer (MODIS) and field-based Forest Inventory and Analysis (FIA) data of net primary productivity (NPP) were compared at increasing levels of spatial aggregation across the eastern USA. A total of 52,167 FIA plots and colocated MODIS forest cover NPP pixels were analyzed using a hexagonal tiling system. A protocol was developed to assess the optimal scale as an optimal size of landscape patches at which to map spatially explicit estimates of MODIS and FIA NPP. The optimal mapping resolution (hereafter referred to as optimal scale) is determined using spatially scaled z -statistics as the tradeoff between increased spatial agreement as measured by Pearson's correlation coefficient and decreased details of coverage as measured by the number of hexagons. Spatial sensitivity was also assessed using land cover assessment and forest homogeneity using spatially scaled z -

statistics. Pearson correlations indicate that MODIS and FIA NPP are most highly correlated when using large hexagons, while z -statistics indicate an optimal scale at an intermediate hexagon size of 390 km². This optimal scale had more spatial detail than was obtained for larger hexagons and greater spatial agreement than was obtained for smaller hexagons. The z -statistics for land cover assessment and forest homogeneity also indicated an optimal scale of 390 km².

Keywords Optimal mapping resolution · Optimal scale · NPP · MODIS · FIA · Eastern USA

Introduction

Changes in net primary productivity (NPP) are a key measure of how forest trees (hereafter referred to as forest) respond to climate change: an increase in NPP would increase the uptake of the atmospheric carbon and thus decrease current warming trends, while a decrease of NPP would reduce the capacity of forests to sequester carbon and thus reinforce current warming trends (Zhao and Running 2010). The monitoring of forest carbon balance can be facilitated by the analysis of spatially explicit maps of NPP (Tang et al. 2010).

The data employed for such map-based monitoring on NPP include forest inventories (Brown and Schroeder 1999; Jenkins et al. 2001), remote sensing (Pan et al. 2006; Turner et al. 2004), and ecosystem

Y. Kwon (✉)
Department of Geography, University of Delaware,
125 Academy Street,
Newark, DE 19716, USA
e-mail: ykwon@udel.edu

C. P. S. Larsen
Department of Geography, University at Buffalo, The State
University of New York,
Buffalo, NY 14261, USA

models (Coops et al. 1998; Waring et al. 2010). Although there has been much work to have the measures from these different methods converge (Potter et al. 2008; Zhang and Kondragunta 2006; Baldocchi 2003), inherent scaling mismatches in the drivers of NPP make this challenging. For example, field methods that employ small inventory plots will be more sensitive to local drivers such as site conditions and forest management (Bettinger et al. 2009), while remote sensing methods will be more sensitive to regional drivers such as climate change (Gotway and Young 2002; Zhao et al. 2006) because they have been parameterized to match climate (Loehle and LeBlanc 1996). For example, the remotely sensed Moderate Resolution Imaging Spectroradiometer (MODIS) and field-based US Forest Inventory Analysis program (FIA) data are the two most frequently employed data sources for regional NPP analysis, yet they have different spatial resolutions at which their NPP signals are observed. The mismatch is that, while MODIS provides its data in a spatially contiguous square grid with a 1-km² pixel resolution, FIA data has spatial sampling intensity of one plot for every 24.3 km², with that plot itself having a total area of 0.0041 km² (McRoberts et al. 2005).

One solution to this mismatch is to recognize that, as field and remote sensing records contain unique elements in their records of NPP, both records should be employed in monitoring of C sequestration (Lu 2006). The application of such a joint monitoring first requires, however, the identification of the optimal scale considering both magnitude of study (i.e., geographic extent) and degree of detail (i.e., its level of geographic resolution) at which the data should be mapped (Wu and Li 2009). The *optimal scale* in this study refers to the optimal geographic mapping resolution at which to publish and use different spatial data resolutions that can provide both local details by finer resolutions and regional trends by coarse resolutions.

The choice of the minimum mapping unit (MMU) has been a fundamental issue in the development of mapping frames for the monitoring of NPP, as the use of different MMUs can result in different spatial patterns of statistical relations (Jelinski and Wu 1996; Ahl et al. 2005). For example, Ahl et al. (2005) reported a difference of up to 7 % in the estimated NPP when the data was scaled up from a 15- to 1-km resolution. Although many ecological studies have examined scaling effects on landscape metrics (e.g., Bian and

Walsh 1993; Wu et al. 2000; White et al. 1992), their settings have typically been limited to a single data source, a narrow range of scales, and few indices. Thus, a comprehensive multiscale analysis using real data is still needed to assess the optimal MMU to assess the site-specific relations between MODIS and FIA NPP.

One approach to choosing the MMU is to simply use the minimum spatial data resolution, as is done in most remote sensing research. This does not provide us with a simple solution because, while MODIS has a data resolution of the 1-km² pixels, for FIA, it could be considered to be an individual tree, an individual plot with an average area of 650 m², an individual representative plot area of 24.3 km², or all plots in a county as it is at the county scale that the FIA has set its standard measurement error of 5 %.

A second approach to choosing the MMU would be to aggregate each NPP dataset to many different MMUs and statistically determine the scale at which the two datasets are most strongly correlated. It might be expected that this would occur at some intermediate size of MMU as FIA contains very local-scale information not present in the MODIS data. However, when the MMU includes data from progressively larger areas, extreme outlying data observations would be averaged with less extreme observations, typically resulting in progressively larger correlations between the two datasets. This scaling effect of geospatial datasets, part of the modifiable areal unit problem (MAUP) formalized by Openshaw and Taylor (1979), has been considered to be an inherently insoluble problem (Cirincione 2000).

A third approach to choosing the MMU, which builds on the statistical approach and solves the scale effect of the MAUP, is to choose the optimal scale through the use of a spatially scaled *z*-statistic. These have been used to select the optimal scale for individual variables (Knight and Lunetta 2003), though it has been suggested that results would be more robust if multiple data types were employed (Riemann et al. 2010). This method resolves the scale effect of the MAUP because, although the correlation should continue to increase with MMU size, the *z*-statistic is calculated by dividing that value by the sample size. Thus, an intermediate MMU should be obtained at which the agreement between the FIA and MODIS NPP datasets and the number of mapping units are both high.

A fourth approach to choosing the MMU would be to find scale at which spatial patterns of forest properties are most sensitive. It is possible that some spatial patterns of forest properties might not change over some range of MMUs but then change when a scale threshold is reached (Hay et al. 2001; Wu 1999; Meentemeyer 1989).

The primary objective of this study is to facilitate the monitoring of forest carbon sequestration in the eastern USA by determining the optimal scale at which to map both MODIS and FIA NPP. We develop a protocol for assessing FIA and MODIS NPP data at increasing multiple spatial scales. First, the geographic patterns of NPP will be examined by creating spatially explicit maps of MODIS NPP and FIA NPP. Second, scaling effects related to the MAUP will be assessed by forest properties that influence calculations of NPP. Third, the optimal scale for the mapping of NPP in the eastern USA will be assessed using an approach which optimizes both the multiple measures of agreement between the MODIS and FIA NPP datasets and the number of mapping units.

Material and methods

Study area and basic mapping frame

The study area is the 31 easternmost US states. We used hexagonal grid system for the basic mapping frame. The hexagonal grid framework, originally used in the Forest Health Monitoring (FHM) program, systematically aggregates plots and pixels independently from potentially regularly spaced landscape features. The hexagons were derived by tessellation from the FHM hexagons that had been used as the basis for the FIA sampling design (McRoberts et al. 2005). In this research, a grid of 648 km² hexagons, originally tessellated from the FHM's hexagonal grid, was obtained from White et al. (1992). A total of five scales of hexagonal frames, built out from the center of the 648-km² hexagons, were created, with 160, 210, 390, 648, and 1,289 km².

FIA database

The publicly available Forest Inventory and Analysis Database (FIADB 4.0), collected by the FIA program

of the Forest Service, US Department of Agriculture was obtained for the 31 easternmost US states. The FIA has achieved significant improvements under the current annual inventory system in timeliness of data acquisition and data comparability. The locational accuracy issues related to “perturbed” and “swapped” plot data (McRoberts et al. 2005) will be negligible in this study since plots are aggregated to large estimation areal units.

Plot-level FIA NPP

Net annual growth was calculated using the interval between two inventories. The individual tree-level estimates of gross annual volume increments were expanded to a per acre value by multiplying them by tree per acre values. The gross annual volume increments of growing-stock trees in the unit of volume per acre (G_i) was, following McRoberts et al. (2005), calculated as (Eq. 1):

$$G_i = \sum_j^4 \sum_t y_{ijt} / \sum_j^4 a_{ij} \quad (1)$$

where y_{ijt} is annual gross change in volume (in cubic feet) for tree t on macroplot, subplot, or microplot j of plot i and a_{ij} is the total area (in acre) used to observe the volume increment on plot i . The value of y_{ijt} is computed as $[(V_2 - V_1)/(T_2 - T_1)]$ where V is the volume, T is the year of measurement, and subscripts 1 and 2 denote the past and current measurements, respectively.

The G_i values in cubic feet per acre were then calculated to aboveground live tree biomass (in grams C per square meter) using species-specific and region-specific allometric methods developed by Jenkins et al. (2004) and standard conversion rates for weight per volume and carbon percent (Table 1; Birdsey 1996). Aboveground live tree biomass includes the following tree components: foliage, stem bark, stem wood, and coarse roots. Equations were developed for groups of similar tree species and size, providing the best available estimates of aboveground biomass (Jenkins et al. 2004, 2001), thus best available estimates of aboveground FIA NPP. Forest types varied by different densities (weight per volume) and percentages of carbon contents (Table 1). Forest types not listed in Table 1 were converted using the average of the conversion factors from the appropriate region.

Table 1 Basic conversion factors of weight per volume and percent carbon for major forest types (source: Birdsey 1996)

US region	Forest type	kgm ⁻³	Percent carbon
South	Loblolly pine	469.57	0.531
	Longleaf pine	539.54	0.531
	Oaks and hickories	609.34	0.479
Northeast and mid-Atlantic	Pines	409.54	0.521
	Spruces and firs	369.67	0.521
	Oaks and hickories	609.34	0.498
	Maples, beeches, and birches	609.34	0.498
North Central	Pines	409.54	0.521
	Spruces and firs	369.67	0.521
	Oaks and hickories	609.34	0.498
	Maples and beeches	579.40	0.498
	Aspens and birches	459.49	0.498

A total of 2,006,210 tally trees from 52,167 ground plots were obtained following the application of three

quality control checks. This control check involved: first, excluding newly established plots which could not be used for the computation of growth rates; second, removing plots which were artificially regenerated; and third, excluding FIA NPP values of >1,500 g C m⁻²year⁻¹ that visual examination of a frequency histogram indicated to be outliers.

FIA NPP at five hexagonal scales

The NPP value in each hexagon was scaled up from the FIA plot values within it using a weighted mean where the plot-scale NPP values in a hexagon were weighted by the number of tally trees that a plot contained. This method is based on the work by Kwon and Larsen (2012) who found that the number of tally trees in a plot was the variable that most influenced plot-level and pixel-level relations between FIA and MODIS primary productivity. The mean number of trees in each of the 52,167 FIA plots was calculated using a weighted approach, with the weight factors calculated as (Eq. 2):

$$W_{ij} = \text{number of trees in plot } i / (\text{number of plots in unit } j \times 36.3 \text{ trees}) \tag{2}$$

where W_{ij} is a dimensionless ratio calculated using all plots i in each hexagon j and 36.3 is the mean number of tally trees in the 52,167 FIA plots. The FIA NPP value in each hexagon was then calculated as (Eq. 3):

$$\text{FIA NPP}_j = \sum_j^n \text{NPP}_{ij} \times W_{ij} \tag{3}$$

where FIA NPP_j was measured in grams C per square meter of forest in hexagon j , NPP_{ij} was the NPP from each plot i in each hexagon j , and W_{ij} was the unitless weight factor for plot i in hexagon j .

MODIS data

The MODIS algorithms to derive primary productivity are described in Running et al. (2004). In the MODIS algorithm, briefly, gross primary productivity (GPP) is modeled using Monteith's (1972) radiation use efficiency, autotrophic respiration (AR) is modeled using Biome-BGC model parameters, and then NPP is calculated as GPP minus AR.

Pixel-level MODIS NPP

The 4-year averages (2001–2004) of MODIS NPP pixel-level values were obtained from the Numerical Terradynamic Simulation Group of the University of Montana. The MODIS NPP data are modeled for individual calendar years. Although the MODIS NPP product has been considered to have not been strongly validated (Turner et al. 2006), it has been steadily improved (Heinsch et al. 2006; Zhao et al. 2005). The improvements include modification of Biome Parameter Look-Up Table based on the 12 flux tower measurements (Zhao et al. 2005) and enhanced interpolation of coarse resolution meteorological input data with temporal filling of cloud-free upstream leaf area index (LAI) and fraction of photosynthetically active radiation (FPAR) data (MOD 15). The most recent collection (C5, MOD 17) of MODIS NPP was assumed to be of the best quality and was downloaded for this study. Each MODIS pixel was classified using the 14 land cover system employed by MODIS; pixels with any of the 5 forest land covers were retained, while pixels with any of the 9 other land cover types were set to null.

MODIS NPP at five hexagonal scales

The MODIS NPP value in each hexagon was scaled up from individual MODIS pixels as a mean of all pixels located in the hexagon (Eq. 4):

$$\text{MODIS NPP}_j = \sum_i^n \text{NPP}_{ij} / n \quad (4)$$

where MODIS NPP_j was the average NPP in hexagon *j* (in grams C per square meter), NPP_{ij} was the annual NPP (in grams C per square meter) in each pixel *i*, and *n* was total number of forested pixels within each hexagon.

Assessment protocols

We first created a choropleth map at increasing spatial scales to visually inspect the spatial pattern of both MODIS and FIA NPP values. We then employed a spatially scaled Fisher's *z*-transformation (hereafter referred to as *z*-statistic) to examine what would be an optimal scale at which to publish and use both MODIS and FIA datasets. The optimal scale at which to map both MODIS and FIA NPP is here defined as the scale at which there is both high spatial agreement (or sensitivity) between the MODIS NPP and FIA NPP datasets and high spatial detail. The spatial agreement is measured by Pearson's correlation coefficient, and the spatial sensitivity of forest properties is measured by a land cover classification error matrix and FIA species composition. The tradeoff between high spatial agreement (or sensitivity) and high spatial detail provides a solution to MAUP. The *z*-statistic is used as an assessment tool to measure the degree of difference between sequential pairs of Pearson's *r*, of land cover classification accuracy, and of forest homogeneity; spatial detail was measured as the number of hexagons within the study area. Unlike Pearson's *r*, the measures of land cover classification accuracy and forest homogeneity do not have an established distribution and are thus used as heuristic confirmative measures; however, we assumed that the distribution for those confirmative measures after Fisher's transformation should be nearly normally distributed.

NPP distribution in choropleth maps

For the purpose of visual inspection, a choropleth map at each scale was created using classes derived by dividing

the frequency histogram of NPP values into five intervals that each contained an approximately equal number of hexagons. Visual comparisons of the choropleth maps were used to assess the influence of different scales of aggregation on the spatial pattern of NPP.

Correlation analysis

As a primary measure of spatial agreement, the correlation coefficient (Pearson's *r*) between collocated MODIS NPP and FIA NPP hexagons was calculated at the five increasing spatial scales.

Agreement of related forest properties

The potential effect of spatial aggregation on land cover accuracy and FIA compositional homogeneity was assessed because forest density, forest homogeneity, and accuracy of land cover classification had a strong influence on the correlations obtained between MODIS and FIA primary productivity at the plot scale across the eastern USA (Kwon and Larsen 2012). To minimize the influence of areas with low forest cover, at each hexagonal scale, these analyses were restricted to hexagons that contained more than the average number of MODIS pixels and FIA plots per hexagon.

Land cover assessment

FIA plots were organized into three land cover classes using the 28 FIA species group codes. An FIA plot was classified as hardwood or softwood if more than 75 % of both its basal area and number of stems were hardwood or softwood, while plots containing <75 % of one type were classified as mixed forest. FIA hexagons were then classified as hardwood or softwood if more than 75 % of plots within it were hardwood or softwood, while all other hexagons were classified as mixed forest hexagons.

The hexagon-level MODIS land cover classification was conducted in a two-step procedure. First, MODIS pixel-level land cover classes (MOD 12) were put into the same three classes as the FIA plots: softwoods (a combination of the two MODIS evergreen classes), hardwoods (a combination of the two MODIS deciduous classes), and mixed forest. Second, MODIS hexagons were then classified as hardwood or softwood if, respectively, more than 75 % of pixels consisted of hardwood or softwood.

A thematic accuracy of land cover classification was then created to assess the similarity of the MODIS and FIA land cover classifications determined by accuracy error matrix created at each of the five hexagonal scales. The error matrix was created using the aforementioned similarly classified three FIA land cover classes as a reference dataset. The average of each of the individual class accuracy was calculated and the overall accuracy was calculated to account for both map-based and reference-based accuracy as the mean of all of the user's and producer's accuracies at each of the five hexagonal scales.

FIA forest homogeneity

FIA compositional forest homogeneity for individual hexagons was determined in two steps. First, an FIA plot was considered to be homogeneous if any 1 of the 28 species group codes comprised more than 50 % of its total basal area and 50 % of the tree stems. Second, a hexagon was considered to be homogeneous if more than 50 % of the total numbers of the FIA plots within a hexagon were considered to be homogenous. Overall FIA forest homogeneity was calculated as the number of hexagons with homogenous FIA forests divided by the total number of hexagons at each of the five hexagonal scales.

The z-statistic approach for optimal scale

The optimal level of spatial aggregation was determined using a form of the z-statistic (Knight and Lunetta 2003) calculated between sequential pairs of different-sized hexagons. The Pearson's correlation coefficients were calculated between the two datasets

Fig. 1 Choropleth maps, with hexagons classified so that there were equal numbers of hexagons per class, at increasing scales (smallest, middle, and largest) for colocated hexagons of FIA NPP (a, b, c) and MODIS NPP (d, e, f). Color codes marked on the histogram correspond to the colors in the associated map. a FIA NPP at 160 km², b FIA NPP at 390 km², c FIA NPP at 1,289 km², d MODIS NPP at 160 km², e MODIS NPP at 390 km², f MODIS NPP at 1,289 km²

and transformed into the normally distributed *r'* using procedures developed by (Fisher 1921) (Eq. 5):

$$r' = 0.5 \ln|(1 + r)/(1 - r)| \tag{5}$$

The z-statistic was then calculated to compare correlation coefficients as (Eq. 6):

$$z = (r'_1 - r'_2) / \sqrt{\frac{1}{n_1 - 3} - \frac{1}{n_2 - 3}} \tag{6}$$

where correlation coefficients (*r*) were transformed to *r'* (Eq. 5), *n* was the number of plots, and subscripts 1 and 2 represent the criterion for that hexagon size with the highest and lowest correlation coefficients, respectively, and the transformed *r'* has the approximate variance of $V(r')=1 / (n-3)$.

For the confirmative measures, the z-statistics were calculated by replacing the numerators in the equation with overall accuracy of classification and FIA forest homogeneity, respectively.

Results

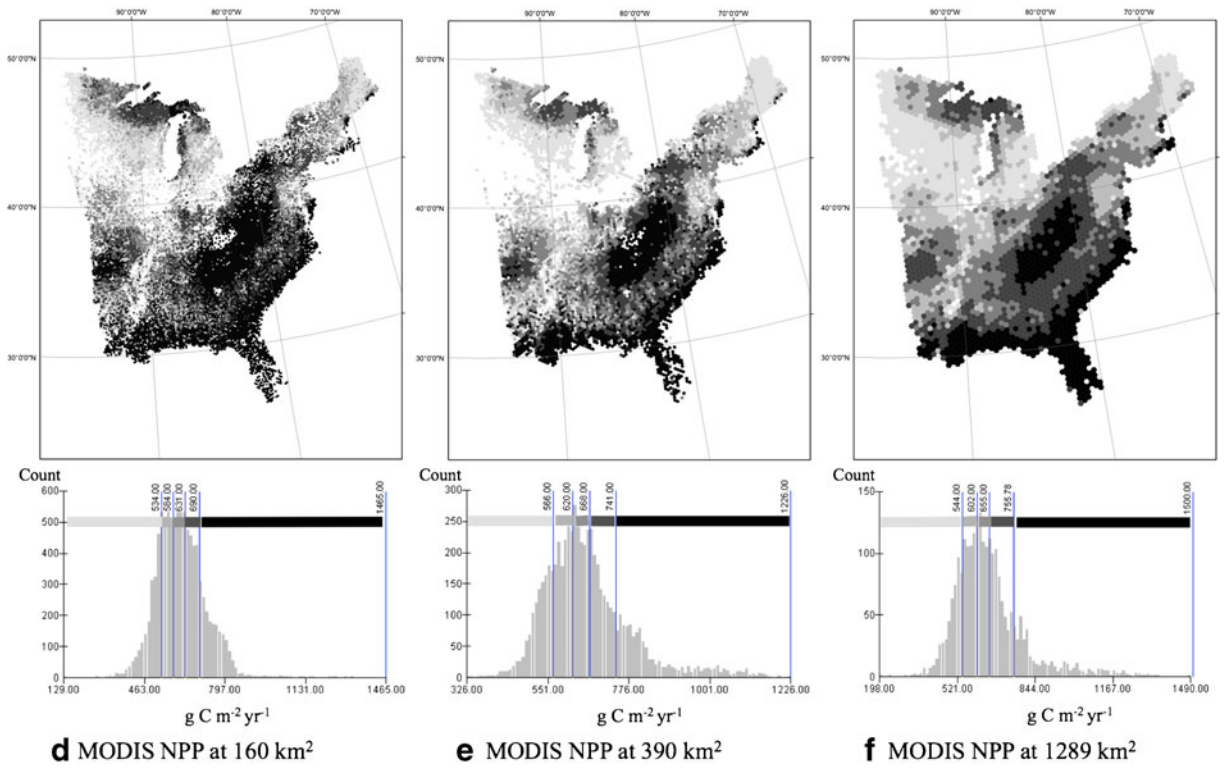
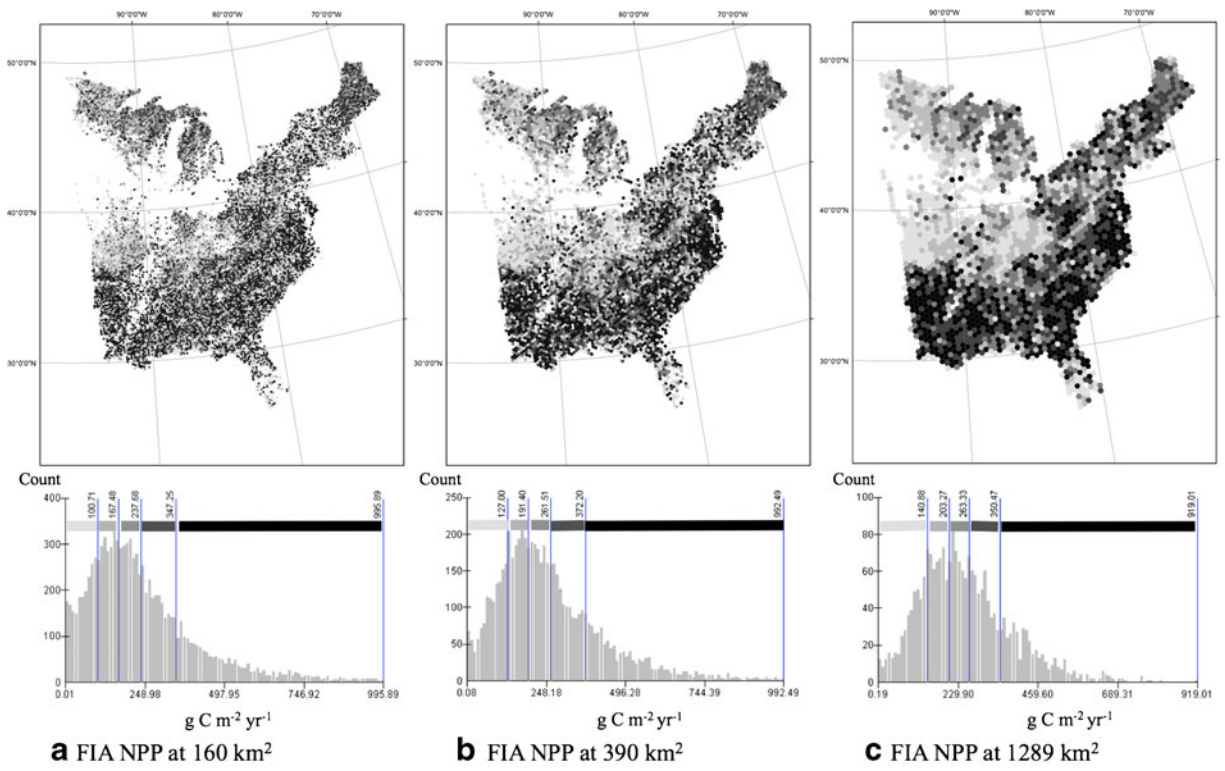
NPP distribution in choropleth maps

The NPP values for all five hexagon sizes were much higher for MODIS than for FIA NPP (Table 2). The

Table 2 MODIS and FIA NPP values for five hexagon sizes

Hexagon sizes (km ²)	No. of colocated hexagons	MODIS NPP (g C m ⁻²)		FIA NPP (g C m ⁻²)		MODIS NPP – FIA NPP (g C m ⁻²)		
		Mean	SD	Mean	SD	Mean	Max	Min
160	13,078	661	149	216	183	445	1,483	-853
210	10,670	660	146	236	177	424	1,455	-830
390	6,443	657	140	271	163	386	1,424	-750
648	4,145	655	138	282	152	373	1,442	-732
1,289	2,250	654	132	297	139	357	1,394	-604

The maximum and minimum values reported for the subtraction of FIA NPP from MODIS NPP are for individual hexagons



mean of FIA NPP increased with hexagon sizes from 216 g C m⁻² for the smallest hexagons to 297 g C m⁻² for the largest hexagons. The mean of MODIS NPP showed a progressive but small decrease from 661 g C m⁻² for the smallest hexagon size to 654 g C m⁻² for the largest hexagon size. As a result, the mean difference was 357 g C m⁻² for the largest hexagons and increased progressively with decreased hexagon size to 445 g C m⁻² for the smallest hexagons. At all scales, there was at least one hexagon in which the MODIS NPP was at least 1,394 g C m⁻² more than the FIA NPP and another hexagon in which the MODIS NPP was at least 604 g C m⁻² less than the FIA NPP.

The general spatial pattern exhibited by both MODIS and FIA was high NPP in the south along an arc from coast areas of the eastern USA to Louisiana and low NPP in the midwest and the north (Fig. 1). A high NPP in the coast areas of the eastern USA for both datasets, in general, can be explained by coast regions being more humid than the inland. For MODIS estimates, an additional reason is that, because the MODIS NPP algorithm uses coarse resolution of global meteorological data, coastal grid cells contain ocean and terrestrial conditions. The inclusion of ocean conditions lowers the apparent vapor pressure deficit (Zhao et al. 2006) and thus raises the MODIS NPP estimates. A latitudinal gradient in NPP was more apparent for MODIS than for FIA NPP at all five hexagonal sizes, as FIA exhibited a more scattered geographic pattern than MODIS. Aggregation of data into larger hexagons made geographic patterns more apparent for both MODIS and FIA.

The FIA NPP exhibited its highest values scattered throughout the south and east, while for MODIS NPP, the highest values exhibited a cluster along the coastline of the south and east and a cluster in the southern Appalachians. The lowest FIA and MODIS NPP values were concentrated in a right-angle triangle that stretched between northern Minnesota and northern Arkansas on the western edge to western North Carolina in the east. Additional small clusters of low NPP were evident for MODIS in northern Maine and for FIA in Florida.

The histograms of the NPP values indicate that increasing spatial aggregation resulted in smoothed distributions for both datasets (Fig. 1). The direction of smoothing effects was different, however, in that MODIS NPP values were averaged towards the outer classes, while FIA NPP values were averaged towards the center classes. In addition, the right tail

of the FIA NPP histogram becomes more positively skewed for larger hexagons, thus increasing the mean FIA NPP, while the symmetric shape of the MODIS NPP histogram was not much affected by scale changes.

Correlation between MODIS and FIA NPP

The collocated FIA and MODIS NPP hexagons exhibited progressively higher, statistically significant, Pearson correlation coefficients for progressively larger hexagon sizes (Table 3). The Pearson's *r* ranged from a low of 0.12 at a hexagon size of 160 km² to a high of 0.34 at a hexagon size of 1,289 km².

Agreement of related forest properties

Land cover assessment

The three land cover classes showed similar spatial patterns for both FIA and MODIS classifications (Fig. 2). The classes exhibited four major clusters that arced from the southwest to the northeast in the following sequence from south to north: softwood and evergreen primarily in Florida, mixed wood, hardwood and deciduous, and mixed wood. MODIS classes exhibited more spatial aggregation of individual covers than FIA classes.

The softwood cover class was the least abundant class in all sizes of hexagons, for both MODIS (6 to 9 %) and FIA (4 to 8 %), as calculated using the pixel and plot numbers in Table 4. For MODIS, hardwoods

Table 3 Correlations between collocated MODIS and FIA NPP hexagons for five sizes of hexagons

Hexagon size	Number of FIA hexagons	Number of MODIS hexagons	Number of collocated hexagons	Pearson's <i>r</i>	<i>z</i> value
160	15,161	15,794	13,078	0.12	–
210	12,178	12,828	10,670	0.14	1.97
390	7,315	7,253	6,443	0.24	6.31
648	4,645	4,532	4,145	0.30	3.25
1,289	2,452	2,459	2,250	0.34	1.64

The *z* values are for comparisons between the hexagon size for which the *z*-value is given and the adjacent smaller hexagon size. All Pearson's correlations are significant at $p < 0.0001$. The *z* values were significant at $p < 0.001$ for the all pairs of hexagon sizes, except hexagon sizes between 648 and 1,289 km² ($p = 0.1$)

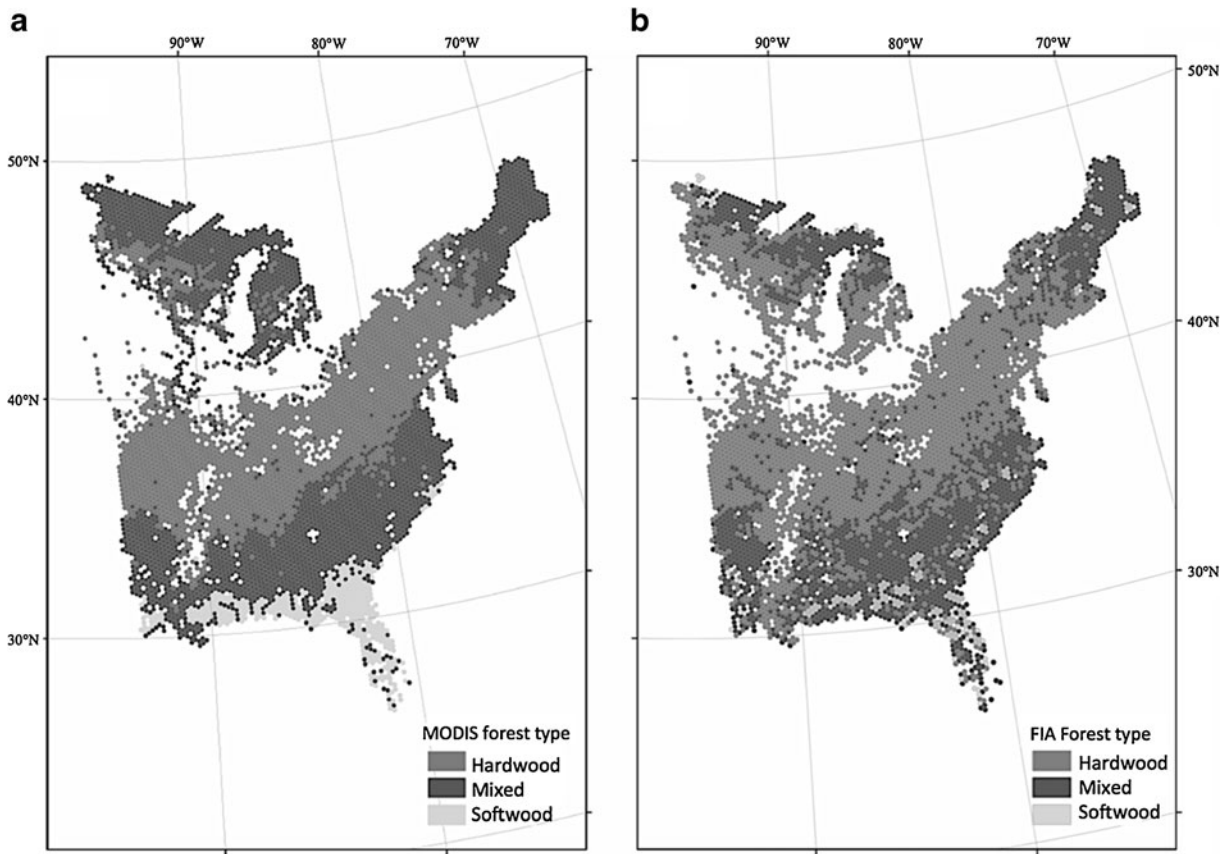


Fig. 2 Land cover classes for MODIS (a) and FIA (b) using a hexagon size of 390 km²

were intermediate in abundance (33 to 39 %) and mixed woods were most abundant (54 to 58 %), while the opposite was the case for FIA where mixed woods were intermediate in abundance (40 to 44 %) and hardwoods were most abundant (48 to 55 %). For the FIA data, the abundance of hardwoods increased progressively from 48 % in the smallest hexagons to 55 % in the largest hexagons, while for MODIS, it increased from 32 to 39 %. The user's accuracy increased steadily for hardwood and mixed forests as the hexagon sizes became progressively larger than 210 km², while that for softwood classes decreased. The producer's accuracy increased for all types as the hexagon sizes increased. The overall accuracy was lowest for the smallest hexagon size and generally increased with increasing hexagon size (Table 4).

FIA forest homogeneity

The percentage of hexagons that contained more than average number of plots increased steadily from 32 %

for the smallest hexagon size to 41 % for the largest hexagon size (Table 5). The proportion of FIA hexagons that were homogenous decreased steadily from 28.6 % for the smallest hexagons to 11.1 % for the largest ones (Table 5).

The z-statistic approach for optimal scale

The *z*-statistics for spatial agreement measured by Pearson's *r* peaked at 6.31 for the hexagon size of 390 km² and decreased steadily as the hexagon size was further increased. The *z*-statistics for confirmative spatial sensitivity measured by overall land cover accuracy and FIA forest homogeneity all peaked at a hexagon size of 390 km² (Fig. 3). The *z*-statistics were largest for FIA homogeneity, intermediate for Pearson's *r*, and lowest for land cover accuracy. The *p* values for all *z*-statistics were <0.001 under the assumption that all three measures have the same distributions of Pearson's *r* for which this test is designed.

Table 4 Land cover assessment error matrix at increasing five spatial scales

Hexagon size (km ²)		MODIS land cover	FIA land cover				User's accuracy
			Hardwood	Softwood	Mixed	Totals	
MODIS	160	Hardwood	1,394	3	167	1,564	89.1
		Softwood	30	76	310	416	18.3
		Mixed	857	277	1,643	2,777	59.2
		Totals	2,281	356	2,120	4,757	–
		Producer's accuracy	61.1	21.3	77.5		
		Overall accuracy (%)	65.4				
	210	Hardwood	1,174	4	196	1,374	85.4
		Softwood	29	63	117	209	30.1
		Mixed	709	253	1,177	2,139	55.0
		Totals	1,912	320	1,490	3,722	–
		Producer's accuracy	61.4	19.7	79.0		
		Overall accuracy (%)	64.8				
	390	Hardwood	761	1	80	842	90.4
		Softwood	8	39	85	132	29.5
		Mixed	414	114	802	1,330	60.3
		Totals	1,183	154	967	2,304	–
		Producer's Accuracy	64.3	25.3	82.9		
		Overall accuracy (%)	69.5				
	648	Hardwood	627	1	55	683	91.8
		Softwood	5	31	73	109	28.4
		Mixed	325	59	606	990	61.2
		Totals	957	91	734	1,782	–
		Producer's accuracy	65.5	34.1	82.6		
		Overall accuracy (%)	70.9				
	1,289	Hardwood	363	0	18	381	95.3
		Softwood	1	14	42	57	24.6
		Mixed	168	24	339	531	63.8
		Totals	532	38	399	969	–
		Producer's accuracy	68.2	36.8	85.0		
		Overall accuracy (%)	73.9				

For each hexagon size, the only hexagons that were employed were those that had more than average number of pixels and plots per hexagon

Discussion

Optimal scale

Pixel-level MODIS validation with plot-level field measurement has been problematic for the following reasons: <30 % of pixels are at-nadir observations (Tan et al. 2006), the modeled estimates of primary productivity were derived from inputs with a variety of spatial resolutions (Running et al. 2004), and the

canopy radiation transfer model used to derive the MODIS 1-km FPAR/LAI is a probability model that showed higher accuracy at larger patch scales (Wang et al. 2004).

The optimal mapping unit to employ map-based monitoring of both MODIS and FIA NPP was a hexagon size of 390 km², as this scale had more spatial detail, although a lower correlation, than was obtained for larger hexagons. There was no evidence of scale threshold for transitions in both MODIS and FIA data

Table 5 Homogeneity of FIA data at increasing spatial scales

Hexagon size (km ²)	Number of softwood hexagons	Number of hardwood hexagons	Number of all hexagons	Percent of forest hexagons used	Homogeneity (%)
160	501	882	4,836	32	28.6
210	412	634	3,846	32	27.2
390	190	297	2,691	37	18.1
648	93	150	1,798	39	13.5
1,289	31	80	997	41	11.1

Homogenous hexagons are those in which more than 50 % of the plots within it are considered homogenous. A plot is considered homogenous if any of the 28 species group codes within it made up more than 50 % of the total basal area and 50 % of all tree stems. For each hexagon size, only hexagons that had more than the average number of pixels and plots at that spatial scale were employed

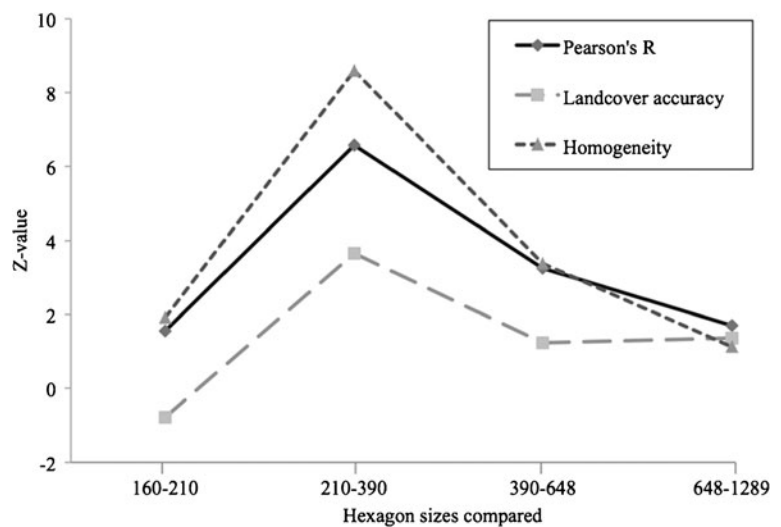
as we see constant NPP changes with scale changes. The 390 km² of the optimal hexagon size was not surprising since it was larger than the mean FIA interplot distance of 4.9 km (McRoberts et al. 2005) and smaller than the MODIS meteorological input variables which have a resolution of approximately 14,000 km² (Running et al. 2004).

Our results suggest that other studies may want to consider the scaling agreement among their various input variables when they consider the spatial resolution at which they will be analyzed. Thus, although model-based predictions of NPP have typically had their output spatial resolution to be equal to the sensor's pixel resolution (Blackard et al. 2008), it is likely that inconsistent spatial resolution of input data may create a major source of variability in model predictions. A different scale problem may influence the result of field-based estimates of biomass conducted at the scale of US states (Zhang and Kondragunta

2006). The high correlations ($R^2=0.58$) obtained in that study between FIA biomass and model estimation may result from the scale effect of the MAUP, making them inappropriate to compare with the size of correlations obtained in studies with a smaller spatial resolution.

The shape of MODIS and FIA data distribution became more dissimilar as the spatial scale of aggregation increased. The histograms for FIA NPP, but not for MODIS NPP, indicated that, as aggregation increased, there was a loss of values in the tails of the distribution. This unusual increase in dissimilarity was also evident in Kolmogorov–Smirnov statistics that found that the most similar empirical cumulative distribution functions were at the smallest scales (results not shown). These differences may be due to the differences in spatial pattern of the two datasets, with MODIS exhibiting more clustering of similarly sized NPP values than did FIA NPP. As a result, aggregation

Fig. 3 The z-statistics calculated for the sequential pairs of hexagons, in order of increasing hexagon sizes



of data into larger hexagons had an opposite effect for MODIS than it did for FIA NPP, with FIA values averaged towards the center of the frequency histogram, while MODIS NPP values were averaged towards both ends.

The confirmative measures of land cover accuracy between MODIS and FIA and FIA forest homogeneity provide greater confidence in the use of correlation-based optimal scale. These measures, however, are for two reasons not completely independent, which may partially explain the similar results. First, because land cover classification is an important constraint in most model-based estimates of NPP because it specifies the physiological properties such as maximum stomata conductance and leaf retention time (Heinsch et al. 2006). MODIS land cover classes were strongly clustered at the regional scale, while the FIA land cover classes exhibited a more scattered distribution throughout the study areas. Since the MODIS land cover classes are used to calculate averaged rate of respiration cost by different biome type properties, the regionalized pattern of land cover classes should thus lead to a regionalized reduction in variance of GPP and NPP. The scattered pattern of FIA land cover classes resulted in increased spatial aggregation, creating an increase in mixed forests and a decrease in FIA forest homogeneity, with this information loss from aggregation of heterogeneous areal units being a recognized geographic problem (Cressie 1993).

Second, forest homogeneity is a key consideration in the stratified sampling methods used by the FIA. Stratification is designed to stratify land into more homogeneous areas to reduce variance of estimation. The importance of homogeneity in terms of accuracy of estimation was also recognized by Bian and Butler (1999) who found that aggregation within the range of spatial autocorrelation produced more predictable statistical and spatial behaviors in homogenous than in heterogeneous areas. Thus, the spatial scale at which forest cover and homogeneity changes will influence the spatial scale over which NPP changes.

It is possible that the inferred optimal scale might be influenced by the difference in size of the pair of hexagons compared. For example, a small difference in hexagon sizes should result in a small change in correlation sizes, land cover accuracy, and homogeneity, while a large difference in size could result in much larger changes. There is some evidence for this in these results with, for example, the increase in

hexagon size from 210 to 390 km² having the second largest increase in size at 86 % and the largest *z*-statistics for all three variables. However, the increase in hexagon size from 648 to 1,289 km² was the largest increase at 99 %, but it had the smallest *z*-statistic for homogeneity and the second smallest for land cover accuracy and NPP. It is possible that the suggested 390 km² is optimal because it reflects FIA sampling resolutions that minimize different sources of errors (i.e., sampling error, measurement error, and allometric error). This issue thus bears more extensive exploration to determine the influence of the change rate in change of spatial scale on the rate of change in *z*-statistics and thus the optimal spatial scale.

Comparisons between MODIS and FIA NPP

Comparability of the modeled values of MODIS NPP and of the field-based values of FIA NPP are indicated by statistically significant correlations that increase with hexagon size and by maps of MODIS and FIA NPP that exhibit similar spatial patterns. However, the correlations between FIA and MODIS NPP are lower than those found between MODIS NPP and measures of NPP from tower-based Bigfoot sites ($R^2=0.40$, Turner et al. 2006), process-based models ($R^2=0.77$, Zhao et al. 2005; $R^2=0.50$, Nayak et al. 2010; $R^2=0.77$, White et al. 2006), and the Finnish national forest inventory ($R^2=0.60$, Muukkonen and Heiskanen 2007). The results for tower-based sites are likely better due to the towers being surrounded by a managed homogeneous forest and because the MODIS and FIA data are compared temporally and not spatially. The results for the process-based models are likely better due to the use of the same radiation input data as MODIS, which means that the two datasets are not independent. The results for the Finnish National Forest Inventory may be better due to a higher sampling intensity within a smaller geographical area than FIA that thus makes them more comparable in scale to the MODIS footprint (Tomppo et al. 2008).

The latitudinal gradient of higher NPP in the south and lower NPP in the north exhibited in the maps of MODIS NPP was also predicted in the nonmapped results of the ecosystem models (Jenkins et al. 1999). While the similarities among ecosystem models likely derive from commonly used broad-scale climatic input sources, differences may be due to different remotely sensed land cover data. For example, the advanced

very high-resolution radiometer (AVHRR) classification for PnET-II identified four forest types (hardwood, spruce–fir, hardwood/pine, and hardwood/spruce–fir), while MODIS identified only three forest types.

Source of uncertainty

The modeled MODIS NPP values are consistently higher than those of FIA NPP. The differences in NPP signals between MODIS and FIA have their own source of uncertainty. The higher mean NPP for MODIS than for FIA was likely due to the differences between NPP components accounted by allometric equations in FIA and biophysical parameters in MODIS algorithm.

In the case of FIA NPP, first, allometric equations might be a major source of uncertainties because the allometric relations should be different for different environments and time periods (Houghton et al. 1999), but they are only different for three regions. Second, there are missing components of NPP that are not covered by this study. These missing components in FIA NPP are litter fall, fine roots, forest floor seedlings and saplings (i.e., stems <12.5 cm diameter at breast height), and understory herbaceous plants. The missing components of litter fall and fine roots should result in an underestimation of FIA NPP by approximately 60 % (Jenkins et al. 2001), while the missing components of forest floor and understory might underestimate ecosystem carbon pools by approximately 7 and 2 %, respectively (Shifley et al. 2012). These missing components, taken together, would result in FIA NPP underestimating MODIS NPP by 69 %, which is in close agreement with FIA NPP in our study being 67 % lower than MODIS NPP.

In the case of MODIS NPP, the major source of uncertainty might be from the remotely sensed MODIS input of LAI, which has a very narrow range within the forest, thus having very limited ability to distinguish different stages of stand size or ages among the same forest type. The assumption made by the MODIS algorithm that live woody mass is related to annual maximum leaf mass seemed somewhat artificially reduced the biomass variance, especially when compared with field-measured biomass data (results not shown). It should be also noted that the saturation problem in GPP (Kwon and Larsen 2012) could influence measures of MODIS NPP that can produce even higher NPP in areas with high GPP,

as tower-based validation for MODIS NPP reported a general tendency of overestimation (Zhao and Running 2011) and especially strong overestimation in cold and dry regions such as occur in high latitudes (Turner et al. 2006).

References

- Ahl, D. E., Gower, S. T., Mackay, D. S., Burrows, S. N., Norman, J. M., & Diak, G. R. (2005). The effects of aggregated land cover data on estimating NPP in northern Wisconsin. *Remote Sensing of Environment*, 97(1), 1–14. doi:10.1016/j.rse.2005.02.016.
- Baldocchi, D. D. (2003). Assessing the eddy covariance technique for evaluating carbon dioxide exchange rates of ecosystems: Past, present and future. *Global Change Biology*, 9(4), 479–492. doi:10.1046/j.1365-2486.2003.00629.x.
- Bettinger, P., Clutter, M., Siry, J., Kane, M., & Pait, J. (2009). Broad implications of southern United States pine clonal forestry on planning and management of forests. *International Forestry Review*, 11(3), 331–345.
- Bian, L., & Butler, R. (1999). Comparing effects of aggregation methods on statistical and spatial properties of simulated spatial data. *Photogrammetric Engineering and Remote Sensing*, 65(1), 73–84.
- Bian, L., & Walsh, S. J. (1993). Scale dependencies of vegetation and topography in a mountainous environment of Montana. *The Professional Geographer*, 45(1), 1–11. doi:10.1111/j.0033-0124.1993.00001.x.
- Birdsey, R. (1996). Carbon storage for major forest types and regions in the conterminous United States. *American Forests*, 2, 261–371.
- Blackard, J. A., Finco, M. V., Helmer, E. H., Holden, G. R., Hoppus, M. L., Jacobs, D. M., et al. (2008). Mapping US forest biomass using nationwide forest inventory data and moderate resolution information. *Remote Sensing of Environment*, 112(4), 1658–1677. doi:10.1016/j.rse.2007.08.021.
- Brown, S. L., & Schroeder, P. E. (1999). Spatial patterns of aboveground production and mortality of woody biomass for eastern US forests. *Ecological Applications*, 9(3), 968–980.
- Cirincione, C., Darling, T., & O'Rourke, T. (2000). Assessing South Carolina's 1990s congressional districting. *Political Geography*, 19(2), 289–211.
- Coops, N. C., Waring, R. H., & Landsberg, J. J. (1998). Assessing forest productivity in Australia and New Zealand using a physiologically-based model driven with averaged monthly weather data and satellite-derived estimates of canopy photosynthetic capacity. *Forest Ecology and Management*, 104(1–3), 113–127.
- Cressie, N. (1993). *Aggregation in geostatistical problems (Geostatistics Troia '92)*. Dordrecht: Kluwer Academic.
- Fisher, R. A. (1921). On the "probable error" of a coefficient of correlation deduced from a small sample. *Metron*, 1, 3–32.

- Gotway, C. A., & Young, L. J. (2002). Combining incompatible spatial data. *Journal of the American Statistical Association*, 97(458), 632–648. doi:10.1198/016214502760047140.
- Hay, G. J., Marceau, D. J., Dube, P., & Bouchard, A. (2001). A multiscale framework for landscape analysis: Object-specific analysis and upscaling. *Landscape Ecology*, 16(6), 471–490. doi:10.1023/a:1013101931793.
- Heinsch, F. A., Zhao, M. S., Running, S. W., Kimball, J. S., Nemani, R. R., Davis, K. J., et al. (2006). Evaluation of remote sensing based terrestrial productivity from MODIS using regional tower eddy flux network observations. *IEEE Transactions on Geoscience and Remote Sensing*, 44(7), 1908–1925. doi:10.1109/tgrs.2005.853936.
- Houghton, R. A., Hackler, J. L., & Lawrence, K. T. (1999). The US carbon budget: Contributions from land-use change. *Science*, 285(5427), 574–578.
- Jelinski, D. E., & Wu, J. G. (1996). The modifiable areal unit problem and implications for landscape ecology. *Landscape Ecology*, 11(3), 129–140. doi:10.1007/bf02447512.
- Jenkins, J. C., Kicklighter, D. W., Ollinger, S. V., Aber, J. D., & Melillo, J. M. (1999). Sources of variability in net primary production predictions at a regional scale: A comparison using PnET-II and TEM 4.0 in northeastern US forests. *Ecosystems*, 2(6), 555–570. doi:10.1007/s100219900102.
- Jenkins, J. C., Birdsey, R. A., & Pan, Y. (2001). Biomass and NPP estimation for the mid-Atlantic region (USA) using plot-level forest inventory data. *Ecological Applications*, 11(4), 1174–1193.
- Jenkins, J., Chojnacky, D., Heath, L., & Birdsey, R. (2004). *Comprehensive database of diameter-based biomass regressions for North American tree species*. Newtown Square: US Department of Agriculture, Forest Service, Northeastern Research Station. (45 pp).
- Knight, J. F., & Lunetta, R. S. (2003). An experimental assessment of minimum mapping unit size. *IEEE Transactions on Geoscience and Remote Sensing*, 41(9), 2132–2134. doi:10.1109/tgrs.2003.816587.
- Kwon, Y., & Larsen, C. (2012). Use of pixel- and plot-scale screening variables to validate MODIS GPP predictions with Forest Inventory and Analysis NPP measures across the eastern USA. *International Journal of Remote Sensing*, 33(19), 6122–6148.
- Loehle, C., & LeBlanc, D. (1996). Model-based assessments of climate change effects on forests: A critical review. *Ecological Modelling*, 90(1), 1–31.
- Lu, D. S. (2006). The potential and challenge of remote sensing-based biomass estimation. *International Journal of Remote Sensing*, 27(7), 1297–1328. doi:10.1080/01431160500486732.
- McRoberts, R. E., Bechtold, W. A., Patterson, P. L., Scott, C. T., & Reams, G. A. (2005). The enhanced forest inventory and analysis program of the USDA Forest Service: Historical perspective and announcement of statistical documentation. *Journal of Forestry*, 103(6), 304–308.
- Meentemeyer, V. (1989). Geographical perspectives of space, time, and scale. *Landscape Ecology*, 3(3–4), 163–173. doi:10.1007/bf00131535.
- Monteith, J. L. (1972). Climate and efficiency of crop production in Britain. *Philosophical Transactions of the Royal Society of London*, 281, 277–294.
- Muukkonen, P., & Heiskanen, J. (2007). Biomass estimation over a large area based on standwise forest inventory data and ASTER and MODIS satellite data: A possibility to verify carbon inventories. *Remote Sensing of Environment*, 107(4), 617–624. doi:10.1016/j.rse.2006.10.011.
- Nayak, R. K., Patel, N. R., & Dadhwal, V. K. (2010). Estimation and analysis of terrestrial net primary productivity over India by remote-sensing-driven terrestrial biosphere model. *Environmental Monitoring and Assessment*, 170(1–4), 195–213. doi:10.1007/s10661-009-1226-9.
- Openshaw, S., & Taylor, P. (1979). A million or so correlation coefficients: Three experiments on the modifiable area unit problem. In N. Wrigley (Ed.), *Statistical applications in the spatial sciences*. London: Pion.
- Pan, Y., Birdsey, R., Hom, J., McCullough, K., & Clark, K. (2006). Improved estimates of net primary productivity from MODIS satellite data at regional and local scales. *Ecological Applications*, 16(1), 125–132.
- Potter, C., Gross, P., Klooster, S., Fladeland, M., & Genovese, V. (2008). Storage of carbon in US forests predicted from satellite data, ecosystem modeling, and inventory summaries. *Climatic Change*, 90(3), 269–282. doi:10.1007/s10584-008-9462-5.
- Riemann, R., Wilson, B. T., Lister, A., & Parks, S. (2010). An effective assessment protocol for continuous geospatial datasets of forest characteristics using USFS Forest Inventory and Analysis (FIA) data. *Remote Sensing of Environment*, 114(10), 2337–2352. doi:10.1016/j.rse.2010.05.010.
- Running, S. W., Nemani, R. R., Heinsch, F. A., Zhao, M. S., Reeves, M., & Hashimoto, H. (2004). A continuous satellite-derived measure of global terrestrial primary production. *BioScience*, 54(6), 547–560.
- Shifley, S. R., Aguilar, F. X., Song, N., Stewart, S. I., Nowak, D. J., Gormanson, D. D., et al. (2012). *Forests of the Northern United States*. Newtown Square: US Department of Agriculture, Forest Service, Northeastern Research Station. (202 pp).
- Tan, B., Woodcock, C. E., Hu, J., Zhang, P., Ozdogan, M., Huang, D., et al. (2006). The impact of gridding artifacts on the local spatial properties of MODIS data: Implications for validation, compositing, and band-to-band registration across resolutions. *Remote Sensing of Environment*, 105(2), 98–114. doi:10.1016/j.rse.2006.06.008.
- Tang, G., Beckage, B., Smith, B., & Miller, P. A. (2010). Estimating potential forest NPP, biomass and their climatic sensitivity in New England using a dynamic ecosystem model. *Ecosphere*, 1(16), art18, doi:10.1890/ES10-00087.1.
- Tomppo, E., Olsson, H., Stahl, G., Nilsson, M., Hagner, O., & Katila, M. (2008). Combining national forest inventory field plots and remote sensing data for forest databases. *Remote Sensing of Environment*, 112(5), 1982–1999. doi:10.1016/j.rse.2007.03.032.
- Turner, D. P., Ollinger, S., Smith, M. L., Krankina, O., & Gregory, M. (2004). Scaling net primary production to a MODIS footprint in support of Earth observing system product validation. *International Journal of Remote Sensing*, 25(10), 1961–1979.
- Turner, D. P., Ritts, W. D., Cohen, W. B., Gower, S. T., Running, S. W., Zhao, M. S., et al. (2006). Evaluation of MODIS NPP and GPP products across multiple biomes. *Remote*

- Sensing of Environment*, 102(3–4), 282–292. doi:10.1016/j.rse.2006.02.017.
- Wang, Y. J., Woodcock, C. E., Buermann, W., Stenberg, P., Voipio, P., Smolander, H., et al. (2004). Evaluation of the MODIS LAI algorithm at a coniferous forest site in Finland. *Remote Sensing of Environment*, 91(1), 114–127. doi:10.1016/j.rse.2004.02.007.
- Waring, R. H., Coops, N. C., & Landsberg, J. J. (2010). Improving predictions of forest growth using the 3-PGS model with observations made by remote sensing. *Forest Ecology and Management*, 259(9), 1722–1729. doi:10.1016/j.foreco.2009.05.036.
- White, D., Kimerling, A. J., & Overton, W. S. (1992). Cartographic and geometric components of a global sampling design for environmental monitoring. *Cartography and Geographic Information Systems*, 19(1), 5–22.
- White, J. D., Scott, N. A., Hirsch, A. I., & Running, S. W. (2006). 3-PG productivity modeling of regenerating Amazon forests: Climate sensitivity and comparison with MODIS-derived NPP. *Earth Interactions*, 10, 1–25.
- Wu, J. (1999). Hierarchy and scaling: Extrapolating information along a scaling ladder. *Canadian Journal of Remote Sensing*, 25, 367–380.
- Wu, H., & Li, Z. L. (2009). Scale issues in remote sensing: A review on analysis, processing and modeling. *Sensors*, 9(3), 1768–1793. doi:10.3390/s90301768.
- Wu, J., Jelinski, D. E., Luck, M., & Tueller, P. T. (2000). Multiscale analysis of landscape heterogeneity: Scale variance and pattern metrics. *Geographic Information Sciences*, 6(1), 6–19.
- Zhang, X. Y., & Kondragunta, S. (2006). Estimating forest biomass in the USA using generalized allometric models and MODIS land products. *Geophysical Research Letters*, 33(9), doi:L0940210.1029/2006g1025879.
- Zhao, M., & Running, S. W. (2010). Drought-induced reduction in global terrestrial net primary production from 2000 through 2009. *Science*, 329(5994), 940–943. doi:10.1126/science.1192666.
- Zhao, M., & Running, S. W. (2011). Response to comments on "Drought-induced reduction in global terrestrial net primary production from 2000 through 2009". *Science*, 333(6046), doi:10.1126/science.1199169.
- Zhao, M., Heinsch, F. A., Nemani, R. R., & Running, S. W. (2005). Improvements of the MODIS terrestrial gross and net primary production global data set. *Remote Sensing of Environment*, 95(2), 164–176. doi:10.1016/j.rse.2004.12.011.
- Zhao, M., Running, S. W., & Nemani, R. R. (2006). Sensitivity of Moderate Resolution Imaging Spectroradiometer (MODIS) terrestrial primary production to the accuracy of meteorological reanalyses. *Journal of Geophysical Research-Biogeosciences*, 111(G1), doi:10.1029/2004jg000004.